Calx, a Na-Ca exchanger gene of *Drosophila melanogaster*

Erich M. Schwarz* and Seymour Benzer[†]

Division of Biology, 156–29, California Institute of Technology, Pasadena, CA 91125

ABSTRACT   We have cloned *Calx*, a gene that encodes a Na-Ca exchanger of *Drosophila melanogaster*. *Calx* encodes two repeated motifs, *Calx-α* and *Calx-β*, that overlap domains required for exchanger activity and regulation. *Calx* has multiple transcripts in adults, including at least one expressed in the retina. The *Calx* genomic locus comprises ≥35 kb between the *Atpα* and *rudimentary-like* genes in chromosomal region 93B. In *Xenopus* oocytes, microinjected *Calx* cRNA induces calcium uptake like that of its homolog, the $3Na^+$-$1Ca^{2+}$ exchanger of mammalian heart. Implications of *Calx-α* motifs for the mechanism of Na-Ca exchange are discussed.

Both animals and protists use cytoplasmic Ca^{2+} (Ca_i^{2+}) as an excitatory signal, suggesting that cells co-opted this ion very early in life's history (1). But excitation cannot recur without Ca_i^{2+} effluxes, and prolonged excess Ca_i^{2+} is lethal (2–5). Cells thus expel Ca_i^{2+} with ATP-driven pumps and Na-Ca exchangers (2). These are complementary: exchangers have a low affinity, but a high capacity, for intracellular calcium; pumps the reverse. Na-Ca exchangers are found in diverse metazoan tissues, including neurons, muscles, kidney, and blood cells (6). Both *Limulus* and *Drosophila* photoreceptors display sodium-dependent calcium export, and may use Na-Ca exchange to return to their resting state after activation by light (7–10).

Despite their ubiquity, genes experimentally proven to encode Na-Ca exchangers have been isolated only from mammals (11, 12); they fall into two classes, based on amino acid identity and stoichiometry of action. The cardiac exchanger (NCX1) trades three extracellular Na^+ ions for one Ca_i^{2+} ion (13). Two other exchangers (NCX2 and NCX3), each expressed in brain and skeletal muscle, have 68–73% identity to NCX1 (14, 15). NCX2 and NCX3 behave similarly to cardiac NCX1 in patch clamps, and thus probably also perform $3Na^+$-$1Ca^{2+}$ exchange (14–16). In contrast, the mammalian retinal exchanger NCKX1, expressed in rod photoreceptors, has only 21–25% identity to NCX1–NCX3, and has $4Na^+$-$1Ca^{2+},1K^+$ stoichiometry (12, 13).

We and others have worked to identify components of *Drosophila* phototransduction by isolating visual cDNAs (17, 18). One such cDNA proved to arise from a *Drosophila* homolog of NCX1, and was the subject of a doctoral thesis of one of us (E.M.S.) in which it was designated *Calx* (19). We describe here, in abbreviated form, the cloning and analysis of the gene. Hryshko *et al.* (20) have used *Calx* in physiological experiments and shown that it has intriguing differences from the mammalian NCX1. Ruknudin *et al.* (21) have subsequently isolated this gene independently.

METHODS

Methods were essentially standard (22). An exhaustive description of all methods is provided by Schwarz (19).

RESULTS

***Calx* cDNAs.** The original *Calx* cDNA, 9C5-o, is from a subtractive cDNA library and is 377 bp long (17). We isolated five more cDNAs from a λgt11 library (23) and sequenced the longest one (9C5-E). A schematic diagram of 9C5-E (5,408 bp) is shown in Fig. 1. Its major ORF of 950 residues (Fig. 2) has a complex pattern of similarities to known or suspected Na-Ca exchangers (Fig. 3). We thus rename 9C5 "*Calx*," and its major ORF's product "CALX." The 5′ untranslated region of 9C5-E has seven minor nonoverlapping ORFs. The major ORF's start site (5′-GTAACCAGCC<u>ATG</u>CA-3′) differs from the *Drosophila* consensus (5′-CACAACCAAA<u>ATG</u>GC-3′; ref. 25). While 9C5-E lacks a poly(A)$^+$ tail, it does have three polyadenylation signals (26) near its oligo(A)$^+$ 3′ terminus. Partial sequencing of 14 other cDNAs revealed five CALX residues subject to alternative splicing by a precise replacement of 5′-CGATGAATTGGCAG-3′ (in 9C5-E) with 5′-TTCCACT-CACTACC-3′ (Fig. 1, ref. 19). They fall in a region poorly conserved between CALX and NCX1-NCX3; indeed, alternate splicing occurs in the same regions of NCX1 and NCX3 as in CALX (27, 28).

***Calx* Tissue Expression.** We tested the transcriptional polarity and tissue specificity of *Calx* by probing RNA blots with strand-specific 9C5-E probes (Fig. 4). Probes antisense to the major 9C5-E ORF revealed multiple transcripts in adult *Drosophila*; probes comprising the same strand as the major ORF yielded no signals, even against 10 μg of poly(A)$^+$ RNA from adult heads (19). *Calx* poly(A)$^+$ RNAs (Fig. 4) include a transcript in both heads and bodies (4.9 kb); a body-specific transcript (4.0 kb); and three head-specific transcripts that appear unaffected by the presence or absence of the visual system (8.2, 9.0, and ≥≈15 kb). A fifth head-specific transcript is enriched in eyeless heads, and thus appears to be primarily expressed outside the visual system (7.0 kb). A sixth transcript (5.6 kb, close in size to 9C5-E) appears to be expressed both within the visual system and elsewhere in the head. Spatially, *Calx* transcripts are ubiquitously present at all embryonic stages from syncytial to organogenesis (19), and in all tissues of the adult head (e.g., neurons: Fig. 5; ref. 19).

Sequence Analysis of the *Calx* ORF. All mammalian Na-Ca exchangers have common features (13). They have two regions of six potential transmembrane sequences, split by a cytoplasmic domain. The first membrane sequence is transient, being proximal to a signal sequence cleavage site. The mature N terminus is followed by one or more extracellular glycosylation sites. The cytoplasmic domain bears many acidic residues; a prominent acid cluster sits at its C terminus. CALX is predicted to possess all of these traits (Fig. 2). Below, we report novel features of CALX and its homologs.
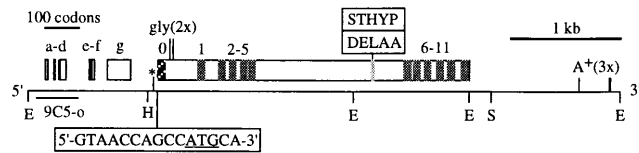
FIG. 1. Features of a *Calx* cDNA, 9C5-E. Along the cDNA's lower side are shown: its overlap with the original 9C5-o clone (17); restriction sites important for subcloning (E, *Eco*RI; H, *Hin*dIII; and S, *Ssp*I); and the sequence context of its major initiation codon (offset box). Above the cDNA, nonoverlapping miniORFs in the 5′ untranslated region (a–g) and the major *Calx* ORF are shown as boxes. Two stop codons immediately 5′ from, and in frame with, the major ORF are marked (*). Within the major ORF, a signal sequence (0) is striped; other transmembrane sequences (1–11) are shaded. Possible *N*-glycosylation sites are marked [gly (2×)]. Residues that vary between cDNAs (19) are shown with light shading and offset boxes above the cDNA; the "DELAA" mini-exon is found in 9C5-E. Three potential polyadenylation signals near the 3′ end of the cDNA are marked [A⁺ (3×)].

Multiple Alignment. We used BLASTP (29) to iteratively screen the nonredundant protein database of the National Center for Biotechnology Information for CALX homologs. We used MACAW (24) to align the homologs in ungapped blocks (Fig. 3). CALX is globally similar to NCX1, NCX2, and NCX3, having 55% identity out of 739 aligned amino acids. Six partial *Caenorhabditis elegans* ORFs and *Xenopus laevis* ORFs have subsets of the NCX1-NCX3 similarities along their lengths; these proteins, with NCX1-NCX3, appear to be CALX orthologs. Ten other proteins appear to be CALX paralogs. They significantly resemble CALX in four ungapped blocks totalling 123 residues: while their identity to CALX in this region is variable (15–37%), in pairwise alignments to CALX they have *P* values of $2 \cdot 10^{-3}$ to $1 \cdot 10^{-14}$ (30). CALX paralogs are found in metazoa, thale cress (*Arabidopsis thaliana*), yeast (*Saccharomyces cerevisiae*), an archaeon (*Methanococcus jannaschii*), and bacteria (*Escherichia coli* and *Synechocystis* PCC6803). While F35C12.2 is 45% identical to NCKX1 (and thus may be its *C. elegans* ortholog), the functions of most CALX paralogs are unknown.

The cytoplasmic domain of NCX1 has three regions defined by deletion analysis (16). The first two enable negative regulation (by an autoinhibitory peptide or elevated intracellular

Na), and mediate high-affinity Ca²⁺ binding (31, 32). The third is required for activation by elevated Ca$_i^{2+}$. The first two regions are well conserved between CALX and NCX1 (61% and 49% identity); the last is less well conserved (33% identity). Accordingly, CALX displays inhibition by autoinhibitory peptide and elevated intracellular sodium, but is partially inhibited by elevated Ca$_i^{2+}$ (20). Protein kinase C stimulates calcium extrusion in *Drosophila* photoreceptors, which significantly depends on Na-Ca exchange (8); similar stimulation has also been seen for NCX1 (33). We checked for protein kinase C substrates conserved between CALX and all of its orthologs. One exists, next to the acid cluster (Figs. 2 and 3) in an NCX1 region not yet tested for function (16).

Intragenic Repeats. We discovered two new motifs in CALX (*Calx-α* and *Calx-β*: Figs. 6–8). While first detected in CALX, they are also reiterated within CALX homologs (Figs. 7 and 8). Their statistical significance is demonstrable by *P* values for aligned pairs of motifs (30). For example, the *Calx-α* motifs of CALX itself have *P* values of $<10^{-3}$ for 57/69 nonidentical pairings with other *Calx-α* motifs and 0.001–0.23 for 12/69 such pairings; those of NCKX1 have *P* values of $<10^{-3}$ for 66/70 such pairings and 0.004–0.03 for 4/70. The *Calx-β* motifs of CALX have *P* values of $<6 \cdot 10^{-6}$ in all nonidentical *Calx-β* pairings.
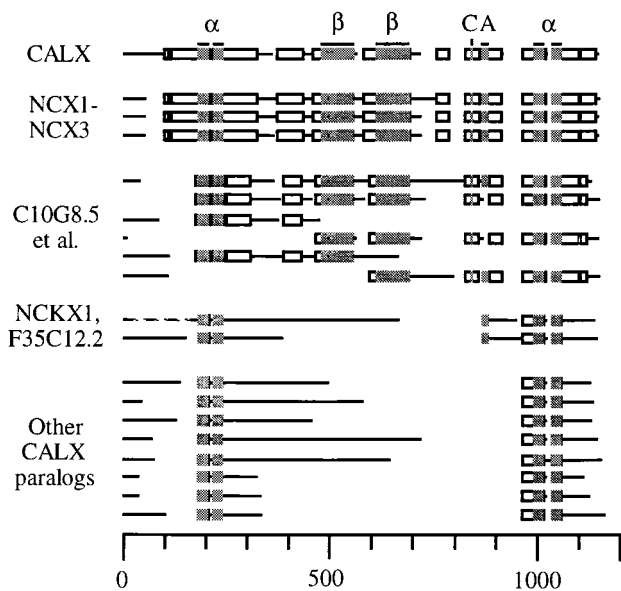

FIG. 3. Schematic alignment of CALX with its homologs. Five groups of sequences are shown, from top to bottom. First is CALX, with conserved motifs indicated above it (α, *Calx-α*; β, *Calx-β*; C, protein kinase C substrate; A, acid cluster). Second are CALX's full-length mammalian orthologs NCX1-NCX3 (all from *Rattus norvegicus*; National Center for Biotechnology Information ID nos. gi|1346652, 1346653, and 1552526). Third are six partial ORFs also orthologous to CALX: C10G8.5, CENACAEX, ZC168.1 [5′], and ZC168.1 [3′] (*C. elegans*: gi|1572830, gi|1009384, gi|1246477, and gi|1246503); XLSOCALX2 and XLSOCALX1 (*X. laevis*: gi|1019101 and gi|1019099). Fourth are NCXK1 (*Bos taurus*: gi|108825) and F35C12.2 (*C. elegans*: gi|1813931). Fifth are paralogs with no clear function: C07A9.4 and C07A9.11 (*C. elegans*: gi|465770 and gi|465776); F7G19.17 (*A. thaliana*: gi|1922938); ORF_D1053 and YJ76_YEAST (*S. cerevisiae*: gi|1429350, gi|1352908); MJ0091 (*M. jannaschii*: gi|1590872); YRBG_ECOLI (*E. coli*: gi|1176841); and slr0681 (*Synechocystis* PCC6803: gi|1652037). Block-aligned regions shown as boxes, and unaligned ones as lines; gaps in the alignment are blank. Bar = residue length. The N terminus of NCKX1 has been truncated. The aligned regions have *P* values of $2.0 \cdot 10^{-4}$ to $<10^{-100}$ (24). Full sequences and references for each homolog are available under its National Center for Biotechnology Information ID no. via the Entrez server (http://www3.ncbi.nlm.nih.gov/Entrez).

<pre>
mglllksiftcalfvifyyatAQSLLKVQETEARQAYLNVTSSSSSNLSQ

DDGHFLSRRLRQVSHGEEGDEGAPSQMDDELEQMTKVHGEAPDAEDVREC
SEGLVLPLWMPQRNISVGDRLVRGFVYFVLLIYLFVGVSIIADRFMAAIE
AITSIERAVVVKGPNNTKQVMHVRIWNETVANLTLMALGSSAPEILLSVI
EIYAKDFESGDLGPGTIVGSAAYNLFMIIAVCMIWIPAGEVRRIRHLRVF
FVTALFSVFAYVWLWLILSVFTPGVILVWEAIVTLLFFPLTVLWAYIAER
RLLVYKMDKNYRVNKRGTVVAGEHDQVEMDAEKGPKQPMVTSARGNDAE
AFDEARREYITLLTELRQKYPDADLEQLEMMAQEQVLARSGRSRAFYRIQ
ATRKMVGSGNLMRKIQERAHSDLTGVKAQLHAGDDEEADDPIRMYFEPGH
YTVMENCGEFEVRVVRRGDISTYASVEYETQDGTASAGTDFVGRKGLLSF
PPGVDEQRFRIEVIDDDVFEEDECFYIRLFNPSEGVKLAVPMIATVMILD
DDHAGIFAFTDSVFEITESVGRFELKVMRYSGARGTVIVPYWTENDTATE
SKDYEGARGELVFENNESEKFIDLFILEESSYEKDVSFKVHIGEPRLAPD
DELAAKIKEVEKKPVQDLTELDRILLLSKPRNGELTTAYVRIRESQEFKA
TVDKLVAKANVSAVLGTSSWKEQFKDALTVIPADESEFDNDDEEEEVPSC
                                                *
FSYVSHFVCLFWKVLFAFVPPTDICGGYVTFVVSIFVIGVITAIIGDAAS
YFGCALNIKDSVTAILFVALGTSIPDTFASMIAAKHDEGADNCIGNVTGS
NAVNVFLGIGLAWTIAAVYHSSHGMTFNVEPGTIGFAVALFCGEALIAIM
LIMFRRWHKGIGAELGGPKVSKYISAAILVFLWVFYVVICILEAYDVIRV
</pre>

FIG. 2. The CALX major ORF. Amino acids are in one-letter code (22). The predicted precursor sequence is shown in lowercase type. Potential *N*-glycosylation substrates in the N-terminal half are underscored with carats. Twelve predicted transmembrane sequences are underlined. Residues identical to a consensus of *Calx-α* or *Calx-β* motifs are in boldface. A conserved protein kinase C substrate and acid cluster are denoted by underscoring with an asterisk and with italics.

Genetics: Schwarz and Benzer
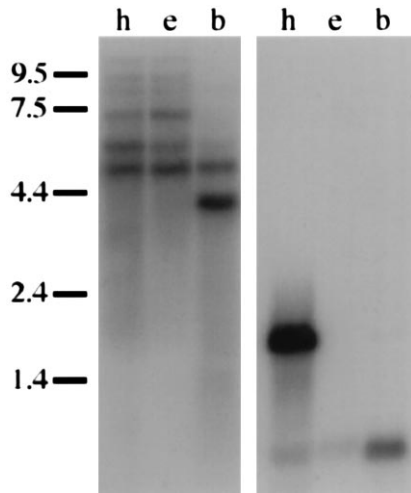
Proc. Natl. Acad. Sci. USA 94 (1997) 10251

FIG. 4. Multiple *Calx* transcripts in adult tissues. In the left autoradiograph, antisense *Calx* probe is seen to hybridize to adult poly(A)$^+$ RNAs. These consist of 5 μg from wild-type heads (h), 5 μg from eyeless (*eyes absent*) heads (e), and 10 μg from mixed-sex wild-type bodies (b). The positions of molecular weight markers are shown alongside the blot (in kb). In adult heads, transcripts with the following sizes are observed: ≥≈15, 9.0, 8.2, 7.0, 5.6, and 4.9 kb. The right autoradiograph is from the same blot as on the left, rehybridized with mixed *ninaE* (rhodopsin) and *RpA1* probes. The retina-specific *ninaE* transcript (1.7 kb) and the ubiquitous *RpA1* transcript (0.68 kb) are both seen.

The *Calx-α* motif is duplicated in all known exchanger homologs, in equivalent locations within both transmembrane regions (Figs. 6 and 7). *Calx-α* motifs are predicted to bridge the membrane, comprising most of transmembrane sequences 2–3 and 8–9. Unlike the *Calx-α* motif, *Calx-β* is only found in exchangers showing global similarity to NCX1–NCX3 (Figs. 3 and 8). Yet an isolated *Calx-β* motif exists in mammalian integrin-β4 and in three *Synechocystis* proteins of unknown function. In both exchangers and mammalian integrins, *Calx-β* motifs are predicted to be cytoplasmic. *Calx-β* motifs are predicted by the PHD neural network (34) to have a series of β-strands and turns (Fig. 8); this is consistent with the *Calx-β* motif being a self-contained β-sheet.

Calx Genomic Region. The *Calx* genomic locus is located in the 93B1,2 doublet of chromosome 3 (N. Bonini, personal communication); it is at least 32 kb long (Fig. 9). It is immediately downstream of the sodium pump α-subunit gene (*Atpα*), also located in 93B1–2 (35). The lethal P insertion P997 was generated in 93B by Wilson *et al*. (37); we mapped its insertion site within *Atpα* (Fig. 9), and found that it failed to complement *l(3)01453* (mapped to 93B1-2 by the Berkeley Drosophila genome project; refs. 19 and 38). We probed *rudimentary-like* genomic phage DNA with a 5.0-kb *Eco*RI fragment from cosmid W5 (just off the 3′ end of the *Calx* region in Fig. 4); it hybridized to a genomic clone proximal to
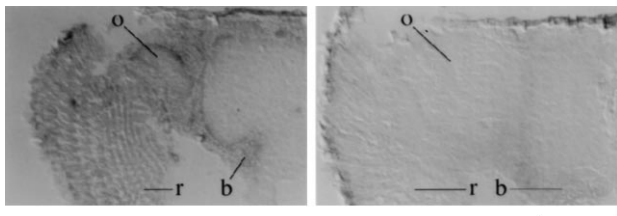

FIG. 5. Spatial pattern of Calx transcripts in the adult head. In the left *in situ* hybridization, digoxigenin-labeled antisense *Calx* probe is seen to hybridize to adult retina (r), optic ganglia (o), and brain (b). In the right *in situ* hybridization, sense (control) *Calx* probe gives only background signals in these tissues. B = 100 μm.
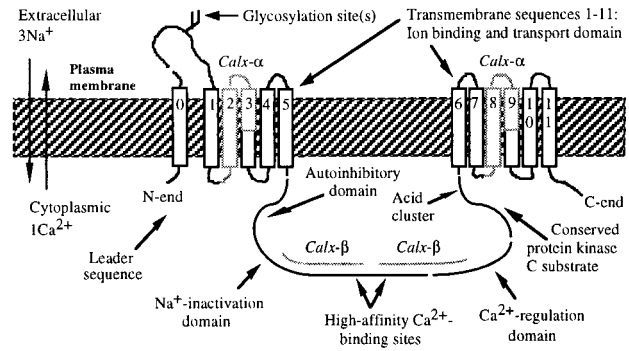

FIG. 6. Schematic diagram of CALX. Ion flows during an outward exchange are shown to the left. *Calx-α* and *Calx-β* motifs map onto regions already known (in NCX1) to be necessary and sufficient for ion transport, high-affinity binding of intracellular calcium, inactivation by elevated intracellular sodium, and autoinhibition (16, 32). The motifs are precisely repeated: the *Calx-α* motifs occupy identical positions within their respective blocks of membrane sequences, while the *Calx-β* motifs are tandem.

rudimentary-like, a UMP synthase gene in 93B6–7 (36). This physically links *Atpα* and *rudimentary-like* via *Calx*, and chromosomally orients both *Calx* and *Atpα* (Fig. 9).

Direct Assays of Na-Ca Exchanger Activity. To directly verify its functional homology to NCX1-NCX3, we assayed

```
CALX       NETVANLTLMALGSSAPEILLSVI--9-GDLGPGTIVGSAAYNLFMIIAV   231
  "        KDSVTAILFVALGTSIPDTFASMI--7-ADNCIGNVTGSNAVNVFLGIGL   861
NCX1       NETVSNLTLMALGSSAPEILLSVI--9-GDLGPSTIVGSAAFNMFIIIAL   182
  "        KDSVTAVVFVALGTSVPDTFASKV--7-ADASIGNVTGSNAVNVFLGIGV   882
NCX2       NETVSNLTLMALGSSAPEILLSVI--9-GELGPGTIVGSAAFNMFVVIAV   179
  "        KDSVNAVVFVALGTSIPDTFASKV--7-ADASIGNVTGSNAVNVFLGLGV   832
NCX3       NETVSNLTLMALGSSAPEILLSLI--9-GDLGPSTIVGSAAFNMFIIIGI   184
  "        KDSVTAVVFVAFGTSVPDTFASKA--7-ADASIGNVTGSNAVNVFLGIGL   838
C10G8.5    NDTVSNLTLMALGSSAPEILLSII--9-GDLGPNTIVGSAAFNLFMIIAI    98
  "        KDAVTAISFVALGTSVPDTFASKV--7-ADNAVGNVTGSNAVNVFLGIGI   821
CENACAEX   NETVSNLTLMALGSSAPEILLSVI--9-GELGPSTIVGSAAFNLFIIIAV    59
  "        KDSVTALTLVAMGTSLPDTFASRT--7-ADGSIGNVTGSNAVNVFLGIGI   668
ZC168.1-5′ NPTVANLTLMALGSSAPEILLSII--9-GDLGPGTIVGSAAFNLFCISAI   143
ZC168.1-3′ KDAVTAITLVALGTSLPDTFASKI--7-ADNAVGNVTGSNSVNVFLGLGL   371
XLSOCALX2  NETVSNLTLMALGSSAPEILLSVI--9-GDLGPSTIVGSAAFNMFVVIAV   167
XLSOCALX1  KDSVTAVVFVALGTSVPDTFASKV--7-ADASIGNVTGSNAVNVFLGIGV   471
Consensus  .-$V$.uT..ALG$$.P-...S.u    .-.o.o.u.GS.A.NuFu.uou

NCKX1      SEDVAGATFMAAGGSAPELFTSLI--6-SNVGIGTIVGSAVFNILFVIGT   536
  "        SEEIMGLTILAAGTSIPDLITSVI--6-GDMAVSSSVGSNIFDITVGLPL  1120
F35C12.2   SDDVAGATFMAAGGSAPEFFTSVI--6-NNVGIGTIVGSATFNILCVLAF   204
  "        PTEIIGLTILAAGTSIPDLITSVI--6-GDMAVSSSVGSNIFDVCVGLPI   523
C07A9.4    SESVAGVTFMAFGNGAPDVFGAIA--9-ADLALGELFGAGLFVTTMVLAV   190
  "        SHEVLGLTILAWSNSIGDLIADVS--6-PRMAMAAAIGGQLFSISPNWIW   522
C07A9.11   SESVAGVTFMAFGNGAPDVFGSIA--9-ADLALGELFGGGLFVTTMVVST    99
  "        SHEVLGLTILAWSNSIGDLIADVS--6-PRMAMAAAIGGPLFNLLMGFGL   515
F7G19.17   SPSMAAVTLLALGNGAPDVFASVA--6-YRTGFGAILSAGTFVSAFVVGF   180
  "        PPALLGLTVLAWGNSVGDLVADVA--6-PAMAMAGCFAGPMFNMLVGLGS   472
ORF_D1053  SDRVSGMTLLALGNALPDITSTYQ--6-TSLAIGELFGGIFFLLTVVIGL   122
  "        SETILGLTIFTWGNSIGDLVSNIT--6-LEIAIGACFGSPLLYFLFGVGF   675
YJ76_YEAST HTGALMAVLLSWCNSSPDLFSNLM-13-VSLSIGEVLGACGIILCIVEGS   133
  "        SKAILGLTIFAWGNSVGDLISNIS-21-FMISCASCLGGVMLNSMGGIGF   629
MJ0091     SNFVIGATVMAIGTSLPEILTSAY--6-PGISIGNAIGSCINIGLVLGL    88
  "        SDKVIGFTLVAFGTSLPELMVSLA--6-GGMVLGNVIGSNIADIGGALAV   247
YRBG_ECOLI PPLIIGMTVVSIGTSLPEVIVSLA--6-RDLAVGTALGSNIINILLILGL    87
  "        SELTMGLTAIAIGTSLPELATAIA--6-NDIAVGNIIGANIFNIVIVLGL   258
slr0681    SPLIIGLTIVAYGTSMPEMVVSLQ--6-ADISIGNVVGSNIFNVLLILGV   154
  "        SELVIGLTLIAAGTSLPELATSVV--6-RDIAVGNVVGSNIFNILAVLGF   327
Consensus  S*.uuGuTuuo.GTSuP-u.$$u      .*uouo..uGo.uFNu...uo.

Notable              P-                      N
```

FIG. 7. Sequence alignment of *Calx-α*. CALX sequences predicted to be membrane-spanning are underlined. Each instance of a motif is shown with: its protein's name; the motif's sequence, with aligned regions separated by indicated numbers of unaligned residues; and the location of the motif's C terminus in the protein. Proteins here are described in Fig. 3. All aligned regions have *P* values of <10^{-100} (24). Residues that match a consensus residue or residue type (shown in the Consensus line) are in boldface type. Residue types are defined as: aromatic (F, W, Y, or H, denoted @); aliphatic (I, L, or V, denoted u); acidic (D or E, −); basic (H, K, or R, +); charged (acidic or basic, ∗); hydroxylic (S or T, $); methyl (A, S, or C, μ), or small (G, A, S, or C, denoted o). A "." denotes sites with no particular consensus. Note that the *Calx-α* motifs of CALX orthologs vs. paralogs have slightly different consensuses. *Calx-α* residues in the "Notable" line are noted in the *Discussion*.

```
Pred. str. LLL...EEEEEEE..LL   EEEEEEE..LLLLLLL   ......   .EEEE.LLL..EEEEEEE..L......   .......

CALX       VMENCGEFEVRVVRRGD-3-YASVEYETQDGTASAG-1-DFVGRK-0-GLLSFPPGVDEQRFRIEVIDDDVFEED-0-ECFYIRL   529
"          ITESVGRFELKVMRYSG-3-TVIVPYWTENDTATES-1-DYEGAR-0-GELVFENNESEKFIDLFILEESSYEKD-0-VSFKVHI   642
NCX1       CLENCGTVALTIIRRGG-4-TVFVDFRTEDGTANAG-1-DYEFTE-0-GTVIFKPGETQKEIRVGIIDDDIFEED-0-ENFLVHL   492
"          VSESIGIMEVKVLRTSG-3-NVIIPYKTIEGTARGG-2-DFEDTC-0-GELEFQNDEIVKTISVKVIDDEEYEKN-0-KTFFIEI   623
NCX2       CLENCGSVLLSVACQGG-4-TFYVDYRTEDGSAKAG-1-DYEYSE-0-GTLVFKPGETQKELRIGIIDDDIFEED-0-EHFFVRL   482
"          VSECMGTVDVRVVRSSG-3-TVRLPYRTVDGTARGG-2-HYEDAC-0-GELEFGDDETMKTLQVKIVDDEEYEKK-0-DNFFIEL   611
NCX3       CLENCGAVLLTVVRKGG-4-TMYVDYKTEDGSANAG-1-DYEFTE-0-GTVVLKPGETQKEFSVGIIDDDIFEED-0-EHFFVRL   484
"          VSESIGVMEVKVLRTSG-3-TVIVPFRTVEGTAKGG-3-DFEDTY-0-GELEFKNDETVKTIRVKIVDEEEYERQ-0-ENFFIAL   618

C10G8.5    VLESVGSFDVVVGRDGG-4-TVMVDYFTEDGSANAG-1-DYIPVK-0-GTLTFYPEDKHQKVTIEVVDDDVFEED-0-EHFYLRL   387
"          VVENCGHLSLQMKRHSG-3-KVIIPFRTVEGTASAD-1-HFEMKE-0-GEIVFEDNQTEALVEIGIVDTEQYERS-0-DYFYIEL   517
ZC168.1    VDATDETVSLKIERKGN-3-KFTVSYATVNGLAKKD-1-NFLFKS-0-ETLQFNPGELHKTISIQLINAANWRPN-0-DVFYVHL    89
"          VKENAGFSRSFVTRRGG-4-PLQVHYETEDVTAKQG-1-DYTAVK-1-GILGFEGQEYEKYIDIDVIDDKMDEKD-0-EAFIIEL   189
CENACAEX   CLENVGDVYLTVKCDRG-6-TVTVHYRTIADTAQAE-1-DFVHTE-0-GTITFEPGQTEQKIKVGIVDNDIYEDD-0-EQFMVRL   355
"          CTESCGSFVAEVIRSRG-3-KVSIPYKTVDGAAKSP-1-DYEHQE-0-GVLKFADEQSKAEIYIPIVNDDEYEKH-0-EDFYIEL   477
XLSOCALX1  [CLENCGTVALTIVRGG]   TVYEDFRTEDGSANAG-1-DYEFTE-0-GTIIFKPGETQKELRVGIIDDDIFEED-0-ENFLVHL    74
"          VSESVGIMEIKVMRTSG-3-TVIVPYKTVEGTARGG-2-DFEDTC-0-GQLEFQNDEIVKTISVKIIDDEEYEKN-0-KTFFLEI   204

int. β4    VSRGDQVARIPVIRHIL-3-KSQVSYSTQDNTAHGH-1-DYVPVE-0-GELLFYPGETWKELQVKLLELQEVDSL-6-RRFQVQL  1085
slr0408    ASEALGEVDFTIERTGD-3-YVVVSYLTQDMDGKAG-1-RYLPVA-0-GQLVFKPGETKKTIKVKVPNDSIYTGD-0-KQFGLLV  3731
slr1403    VKETDGEAVLLVRRTGN-3-AVSFNYRTVDGSATAG-1-DYVAQA-0-GTLTFAPGEVFKEIRIAILDDDITERR-1-EKFRVVI   937
slr1028    VSEAAGEAQFVIERTGD-3-YVLVSYITQDMSGKAG-1-RYLPIA-0-GQLIFNPGENQKNITVKIPTDSVYTAD-0-RQFSLLV  3504

Consensus  u.EooG*u*u.u.R+o.   .u.u.@*T.-G$A+oG   *@...*   G.u.F*..-$*K-u*u*uu---u@-*-   **F.u*u
```

FIG. 8.   Sequence alignment of *Calx-β*. Format, references, and *P* values are as in Fig. 7 unless noted. The N terminus of XLSOCALX1's first *Calx-β* motif is assumed to be residues 400–416 of XLSOCALX2 (in brackets). "Pred. str." denotes secondary structures predicted for *Calx-β* motifs by the PHD neural network (34). "E" and "L" denote residues predicted to be in an extended strand (e.g., a β-strand) or in a loop; those shown here were predicted with 82% accuracy for both N- and C-terminal *Calx-β* motifs. Most proteins here are described in Fig. 3, except for integrin-β4 (*R. norvegicus*: gi|1401303) and slr0408, slr1028, and slr1403 (*Synechocystis* PCC6803: gi|1653629, gi|1652242, and gi|1652714).

CALX by exploiting the reversibility of Na-Ca exchange in *Xenopus* oocytes (11). Capped *Calx* cRNAs were synthesized from pXexCalx, a *Hin*dIII/*Ssp*I subclone of 9C5-E containing the major ORF (Fig. 1). Plasmids encoding NCX1 and the *Drosophila* potassium channel *Shaker* (1) were used as templates for capped NCX1 and *Shaker* cRNAs (16, 39). Finally, we generated a translationally optimized *Calx* cRNA template (PCR-Calx) with PCR. All four templates were used to make standardized aliquots of cRNA.

These cRNAs, in parallel with blank buffer, were microinjected into *Xenopus* oocytes (5 ng per oocyte). After 4–8 days of incubation, these oocytes were loaded with internal Na via nystatin (40), challenged with $^{45}Ca^{2+}$, washed, and assayed for $^{45}Ca^{2+}$ uptake. Calcium uptake was induced by *Calx* cRNAs (Fig. 10). This uptake occurred with external potassium (19) or choline; however, it was absent from oocytes challenged with external sodium, not loaded with internal sodium, or expressing an unrelated ion transporter. While pXexCalx-induced uptake (7 times background) was substantially weaker than that induced by NCX1 (30–35 times background), uptakes comparable to NCX1's were induced by both PCR-Calx (12–19 times background) and 50 ng of pXexCalx cRNA (15–22 times background). Oocytes vigorously expressing exchangers showed some uptake even without sodium loading (Fig. 10). To test whether this might be due to residual sodium within the
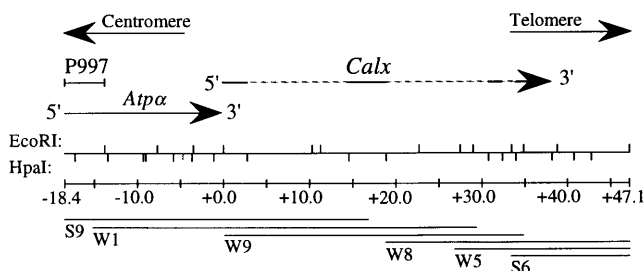

FIG. 9.   The *Calx* genomic region. The topmost line shows genomic DNA; upper ticks mark *Eco*RI sites and lower ticks mark *Hpa*I sites. One *Hpa*I site (at about −5.0 kb) separates two unordered *Hpa*I-*Hpa*I fragments 1.18 and 1.05 kb in size. Above this map, DNA fragments are shown that cross-hybridize to the P997 insertion site, the Na$^+$/K$^+$ pump α-subunit (*Atp*α) gene (35), and *Calx* cDNAs. The proximal end of the *rudimentary-like* genomic walk (36) begins with a 5.0-kb *Eco*RI fragment immediately to the right of the genomic DNA shown here. Chromosomal orientation is shown with arrows. DNA fragments cross-hybridizing to *Calx* cDNA are shown as solid lines; other fragments are stippled. *Calx* transcriptional polarity was deduced from cDNA probes and RNA blots (Fig. 4). Underneath the genomic map are shown distances in kb and six cosmids covering the region.
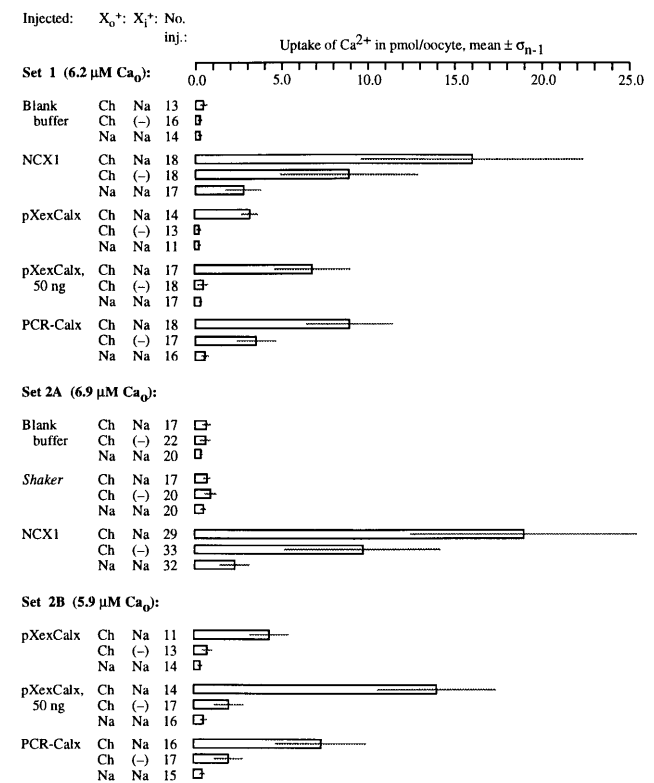

FIG. 10.   Expression of CALX in *Xenopus* oocytes. Sets of oocytes were microinjected, incubated for several days, loaded with intracellular sodium, challenged with $^{45}Ca^{2+}$ along with a variable monovalent cation, and allowed to take up $^{45}Ca^{2+}$ via reverse Na-Ca exchange for 10′. The concentration of $^{45}Ca^{2+}$ used (5.9–6.9 μM) is indicated for each oocyte set. After uptake, oocytes were rinsed and individually assayed by scintillation counting. "Injected" refers to the substance injected; X_o^+, the primary monovalent cation placed outside the oocytes being assayed for $^{45}Ca^{2+}$ uptake; X_i^+, the primary monovalent cation loaded into the oocytes; "No. inj.," the number of oocytes injected with a particular solution; "Uptake of Ca^{2+} in pmol/oocyte, mean ± σ_{n-1}," the mean quantity and SD of $^{45}Ca^{2+}$ taken up per oocyte. "Ch" denotes cationic choline; (−) denotes oocytes left unloaded by outside cations.

oocyte, we loaded *Calx*-expressing oocytes with lithium or potassium cations: these reduced calcium uptake to background levels (19).

DISCUSSION

***Calx-α* and *Calx-β* Motifs: Possible Functions.** Repeated motifs are thought to arise via intragenic duplications, and survive if they improve protein function (41). *Calx-α* motifs are duplicated in all full-length ORFs in which they are found at all, and exist in all three domains of life. This implies both that *Calx-α* motifs arose early in life's history and that their existing as a tandem pair is essential for function. This is consistent with *Calx-α* motifs opposing one another symmetrically across an internal pore spanning the cell membrane (42). Both $3Na^+$-$1Ca^{2+}$ and $4Na^+$-$1Ca^{2+}$, $1K^+$ exchangers (i.e., NCX1 and NCKX1) appear to have two anions that neutralize either Ca^{2+} or $2Na^+$ during the Na-Ca exchange cycle (43, 44). However, no location for such an anion pair has so far been proposed for either NCX1 or NCKX1. Our analysis shows that only one anionic (D or E) residue is completely conserved in all *Calx-α* motifs (Fig. 7). This residue could be one member of a symmetrical pair of two invariant anions flanking the exchanger channel. This D/E residue is invariably adjacent to a helix-breaking residue (generally proline, occasionally glycine; Fig. 7). Such a P/G site could form a constricting bend in the channel, like that of acetylcholine receptors (45). We thus predict these D/E residues to be the two anions used in both $3Na^+$-$1Ca^{2+}$ and $4Na^+$-$1Ca^{2+}$,$1K^+$ exchange. To fully account for its electrogenicity, NCKX1 requires an anion not found in NCX1 (44). One candidate is D_{1113} (Fig. 7): it is predicted to have roughly the same elevation within the membrane as the invariant D/E residues; it is found in the NCKX1 ortholog F35C12.2; and it exists in place of a strongly conserved asparagine residue. In NCX1, homologous residues in N- and C-terminal *Calx-α* motifs have quantitatively similar mutant phenotypes, and mutations of both invariant D/E sites abolish exchange (46). These data are consistent with our model for *Calx-α* function, though more data are needed to test the predictions here.

Extant data support several possibilities for *Calx-β*'s function. NCX1's two *Calx-β* motifs contain a high-affinity Ca_i^{2+}-binding site (Fig. 6; ref. 31). But, because this site only partly encompasses *Calx-β* motifs conserved for $\geq \approx 540$ My (Figs. 3 and 8), the motifs probably have further roles. They overlap a region required for inhibition of NCX1 by elevated intracellular sodium (16); the same region may also bind ankyrin (47). Any of these functions would be appropriate in integrin-*β*4, which connects hemidesmosomes with the cytoskeleton (48) and transduces intracellular signals (49).

1. Hille, B. (1992) *Ionic Channels of Excitable Membranes* (Sinauer, Sunderland, MA), 2nd Ed.
2. Carafoli, E. (1987) *Annu. Rev. Biochem.* **56,** 395–433.
3. Choi, D. W. (1992) *J. Neurobiol.* **23,** 1261–1276.
4. Nicotera, P., Bellomo, G. & Orrenius, S. (1992) *Annu. Rev. Pharmacol. Toxicol.* **32,** 449–470.
5. Cunningham, K. W. & Fink, G. R. (1994) *J. Cell Biol.* **124,** 351–363.
6. Blaustein, M. P., DiPolo, R. & Reeves, J. P., eds. (1991). *Sodium-Calcium Exchange: Proceedings of the Second International Conference* (N. Y. Acad. Sci., New York).
7. O'Day, P. M., Gray-Keller, M. P. & Lonergan, M. (1991) *J. Gen. Physiol.* **97,** 369–391.
8. Ranganathan, R., Bacskai, B. J., Tsien, R. Y. & Zuker, C. S. (1994) *Neuron* **13,** 837–848.
9. Hardie, R. C. (1995) *J. Neurosci.* **15,** 889–902.
10. Ranganathan, R., Malicki, D. M. & Zuker, C. S. (1995) *Annu. Rev. Neurosci.* **18,** 283–317.
11. Nicoll, D. A., Longoni, S. & Philipson, K. D. (1990) *Science* **250,** 562–565.
12. Reiländer, H., Achilles, A., Friedel, U., Maul, G., Lottspeich, F. & Cook, N. J. (1992) *EMBO J.* **11,** 1689–1695.
13. Philipson, K. D. & Nicoll, D. A. (1993) *Int. Rev. Cytol.* **137C,** 199–227.
14. Li, Z., Matsuoka, S., Hryshko, L. V., Nicoll, D. A., Bersohn, M. M., Burke, E. P., Lifton, R. P. & Philipson, K. D. (1994) *J. Biol. Chem.* **269,** 17434–17439.
15. Nicoll, D. A., Quednau, B. D., Qui, Z., Xia, Y. R., Lusis, A. J. & Philipson, K. D. (1996) *J. Biol. Chem.* **271,** 24914–24921.
16. Matsuoka, S., Nicoll, D. A., Reilly, R. F., Hilgemann, D. W. & Philipson, K. D. (1993) *Proc. Natl. Acad. Sci. USA* **90,** 3870–3874.
17. Hyde, D. R., Mecklenburg, K. L., Pollock, J. A., Vihtelic, T. S. & Benzer, S. (1990) *Proc. Natl. Acad. Sci. USA* **87,** 1008–1012.
18. Smith, D. P., Shieh, D.-H. & Zuker, C. S. (1990) *Proc. Natl. Acad. Sci. USA* **87,** 1003–1007.
19. Schwarz, E. M. (1996) Ph.D. thesis (California Institute of Technology, Pasadena).
20. Hryshko, L. V., Matsuoka, S., Nicoll, D. A., Weiss, J. N., Schwarz, E. M., Benzer, S. & Philipson, K. D. (1996) *J. Gen. Physiol.* **108,** 67–74.
21. Ruknudin, A., Valdivia, C., Kofuji, P., Lederer, W. J. & Schulze, D. H. (1997) *Am. J. Physiol.* **273,** C257–C265.
22. Sambrook, J., Fritsch, E. F. & Maniatis, T. (1989) *Molecular Cloning: A Laboratory Manual* (Cold Spring Harbor Lab. Press, Plainview, NY), 2nd Ed.
23. Itoh, N., Salvaterra, P. & Itakura, K. (1985) *Drosophila Inf. Serv.* **61,** 89.
24. Schuler, G. D., Altschul, S. F. & Lipman, D. J. (1991) *Proteins* **9,** 180–190.
25. Cavener, D. R. & Ray, S. C. (1991) *Nucleic Acids Res.* **19,** 3185–3192.
26. Angelichio, M. L., Beck, J. A., Johansen, H. & Iveyhoyle, M. (1991) *Nucleic Acids Res.* **19,** 5037–5043.
27. Lee, S.-L., Yu, A. S. L. & Lytton, J. (1994) *J. Biol. Chem.* **269,** 14849–14852.
28. Quednau, B. D., Nicoll, D. A. & Philipson, K. D. (1997) *Am. J. Physiol.* **272,** C1250–C1261.
29. Altschul, S. F., Boguski, M. S., Gish, W. & Wootton, J. C. (1994) *Nat. Genet.* **6,** 119–129.
30. Pearson, W. R. (1996) *Methods Enzymol.* **266,** 227–258.
31. Matsuoka, S., Nicoll, D. A., Hryshko, L. V., Levitsky, D. O., Weiss, J. N. & Philipson, K. D. (1995) *J. Gen. Physiol.* **105,** 403–420.
32. Matsuoka, S., Nicoll, D. A., He, Z. & Philipson, K. D. (1997) *J. Gen. Physiol.* **109,** 273–286.
33. Iwamoto, T., Pan, Y., Wakabayashi, S., Imagawa, T., Yamanaka, H. I. & Shigekawa, M. (1996) *J. Biol. Chem.* **271,** 13609–13615.
34. Rost, B. & Sander, C. (1994) *Proteins* **19,** 55–72.
35. Schubiger, M., Feng, Y., Fambrough, D. M. & Palka, J. (1994) *Neuron* **12,** 373–381.
36. Eisenberg, M., Gathy, K., Vincent, T. & Rawls, J. (1990) *Mol. Gen. Genet.* **222,** 1–8.
37. Wilson, C., Pearson, R. K., Bellen, H. J., O'Kane, C. J., Grossniklaus, U. & Gehring, W. J. (1989) *Genes Dev.* **3,** 1301–1313.
38. Karpen, G. H. & Spradling, A. C. (1992) *Genetics* **132,** 737–753.
39. Klaiber, K., Williams, N., Roberts, T. M., Papazian, D. M., Jan, L. Y. & Miller, C. (1990) *Neuron* **5,** 221–226.
40. Longoni, S., Coady, M. J., Ikeda, T. & Philipson, K. D. (1988) *Am. J. Physiol.* **255,** C870–C873.
41. Li, W.-H. & Graur, D. (1991) *Fundamentals of Molecular Evolution* (Sinauer, Sunderland, MA)

42. Kyte, J. (1981) *Nature (London)* **292,** 201–204.
43. Hilgemann, D. W., Nicoll, D. A. & Philipson, K. D. (1991) *Nature (London)* **352,** 715–718.
44. Perry, R. J. & McNaughton, P. A. (1993) *J. Physiol. (London)* **466,** 443–480.
45. Unwin, N. (1993) *J. Mol. Biol.* **229,** 1101–1124.
46. Nicoll, D. A., Hryshko, L. V., Matsuoka, S., Frank, J. S. & Philipson, K. D. (1996) *J. Biol. Chem.* **271,** 13385–13391.

47. Li, Z., Burke, E. P., Frank, J. S., Bennett, V. & Philipson, K. D. (1993) *J. Biol. Chem.* **268,** 11489–11491.
48. Spinardi, L., Ren, Y.-L., Sanders, R. & Giancotti, F. G. (1993) *Mol. Biol. Cell* **4,** 871–884.
49. Mainiero, F., Murgia, C., Wary, K. K., Curatola, A. M., Pepe, A., Blumemberg, M., Westwick, J. K., Der, C. J. & Giancotti, F. G. (1997) *EMBO J.* **16,** 2365–2375.